THE RAMAN SPECTROSCOPY USE FOR MONITORING OF CHANGES IN THE GLASS STRUCTURE OF THE THIN LAYERS CAUSED BY ION IMPLANTATION

[#]P. NEKVINDOVA*, B. SVECOVA*, S. STANEK*, S. VYTYKACOVA*, A. MACKOVA**,***, P. MALINSKY**,***, V. MACHOVIC*, J. SPIRKOVA*

*Department of Inorganic Chemistry, Faculty of Chemical Technology, University of Chemistry and Technology, Technicka 5, 166 28 Prague, Czech Republic
**Nuclear Physics Institute, Academy of Sciences of the Czech Republic, v.v.i., 250 68 Rez, Czech Republic
***Department of Physics, Faculty of Science, J. E. Purkinje University, Ceske mladeze 8, 400 96 Usti nad Labem, Czech Republic

[#]E-mail: pavla.nekvindova@vscht.cz

Submitted March 18, 2015; accepted June 24, 2015

Keywords: Glasses; Nano particles; Raman spectroscopy; Ion implantation

In this paper, we have demonstrated the utility of Raman spectroscopy as a technique for the characterisation of changes in the glass structure of the thin layers caused by ion implantation. Various types of silicate glasses were implanted by Au^+ ions with energy of 1.7 MeV and a fluence of 1×10^{16} ions·cm^{-2} to create gold nanoparticles in thin sub-surface layer of the glass. It was proved that the structure of the glass has an indisputable impact on the extent of depolymerisation of the glass network after implantation. It was shown that the degree of glass matrix depolymerisation can be described using the evaluation of Q_n factors in the implanted layers from different depths. After analysis of Raman spectra, the relation between nucleation and the resulting parameters of the gold nanoparticles was put into connection with the feasibility of the glass to recover its structure during post-implantation annealing. Also the creation of new bonds in the glass network was discussed.

INTRODUCTION

Ion implantation is known to be a promising technique for synthesising nanostructured materials in glass [1-4] and for assembling and organising complex nanostructures into advanced devices. In this method, energetic ions are impinged into the sub-surface region of a substrate material and cause the depolymerisation of the glass network [5, 6]. The structure of the glass matrix that has been damaged by the penetration of the implanted ions can be recovered during another technological step – thermal annealing [7-9]. Moreover, the addition of annealing can substantially influence the nucleation and the size of nanoparticles and thus also the parameters of the resulting thin optical layers. However, ion implantation of metal particles into a glass substrate has a crucial problem, namely the control of the structural modification of the glass created by energetic-ion penetration through the glass substrate. Earlier literature used Raman spectroscopy for the characterisation of the structure of ancient glasses [10]. Here we are going to show that Raman spectroscopy can be used for the characterisation of the changes in glass structure caused by ion implantation and post-implantation annealing.

Glass possesses some advantages, which are superior to those of crystals and polymers. In particular, glass composition can be designed and tuned according to the needs of the photonics components encompassed [11]. The changes of the glass composition result in a change of the glass structure. It is well known that the structure of silica glass is random (disordered), consisting of SiO_4 tetrahedrons, which are connected only with the corners but not with the edges or even faces [12, 13]. The addition of alkali oxide into silica glass leads to a network modification, i.e. the breaking of the Si-O-Si linkage and the formation of Si–O$^-$ terminations, which makes the glass structure depolymerised. An oxygen atom linking two tetrahedrons is called a bridging oxygen (BO), whereas an oxygen in Si–O$^-$ is known as a non-bridging oxygen (NBO). The modification of the silicate-glass network results in the formation of several structures, e.g. isolated tetrahedrons, pairs of tetrahedrons linked by a common oxygen atom (Si_2O_7), three tetrahedrons linked by sharing two oxygen atoms (i.e. three (Si_3O_9) and n tetrahedral-cycles), or by sharing three oxygen atoms (e.g. in some chains, ribbons and layers), and structures similar to those in pure SiO_2. New structures are usually marked with the Q_n notation,

where the subscript indicates the number of BOs. It is known that the structure of the glass and Q_n species can be determined by Raman spectroscopy [10].

Ion implantation of Au^+ with an energy of 1.7 MeV and a fluence of 1×10^{16} ions·cm^{-2} along with post-implantation annealing were used to synthesise metal nanoparticles in various types of silicate glasses in this paper. We evaluated the ratios of the areas of the bending and stretching bands in the Raman spectra of four types of silicate glasses before and after ion implantation and post-implantation annealing, respectively, and the spectral Q_n components were analysed using a method described in [10]. A deliberate selection of a different glass matrix and the choice of the same preparation conditions led to a systematic description of the relation between the structure of the glass and the formation of gold nanoparticles. The results from Raman spectroscopy were compared and discussed along with the results of RBS [14, 15], TEM [16] and Z-scan [17] analyses published before.

EXPERIMENTAL

According to our previous experiments [18], four types of glass substrate with different glass-network structures were selected. We used glass substrates with different chemical compositions (see Table 1), namely the specially designed glass type GIL49 and Glass B (made at the Glass Institute Hradec Kralove Ltd., Czech Republic) and commercially available BK7 and silica glass. The glasses varied especially in the concentrations and type of network formers (SiO_2, B_2O_3) and network modifiers (alkali oxides).

Table 1. The composition of the glasses used (at. %).

Type of glass	SiO_2	B_2O_3	Na_2O	K_2O	Other components
BK7	58	18	14	9	As_2O_3, BaO
GIL49	63	–	24	0.5	Al_2O3, CaO, MgO
Glass B	88	–	9	–	Al_2O_3
Silica glass	100	–	–	–	–

The pre-cleaned glass substrates were implanted with Au^+ ions at an energy of 1.7 MeV at the Nuclear Physics Institute, Academy of Sciences of the Czech Republic, with an ion fluence of 1×10^{16} cm^{-2}. The as-implanted glasses were annealed in air at temperature of 600°C for 5 hours.

Raman spectra were collected using a Jobin Yvon model of the Labram HR equipped with a 532 nm line laser, with the power on the head of the laser being 50 mW. An objective with a magnification of 50 times was used to focus the laser beam on the sample. The scattered light was analysed by a spectrograph with a holographic grating of 600 g·mm^{-1}, slit width of 100 μm and confocal hole of 400 μm. The adjustment of the system was regularly checked using a silicon sample. The acquisition time was 20 s, and twenty accumulations were co-added to obtain a spectrum. The beam size of Raman scattering as well as the spatial resolution was 1μm. The device was specially modified to make it possible to focus the beam with a minimum step of 100 nm towards the depth. The Raman spectra were collected from different depths of the implanted layer (i.e. from the sample surface to a depth of 1 mm with a 100-nm step) in the wavelength range of 200 - 1500 cm^{-1}. The obtained spectra were analysed (baseline correction and spectral component analysis) in the OMNIC 7.3 program.

RESULTS

Non-implanted glass substrate

The structure of virgin, non-implanted glasses was characterised by Raman spectroscopy in the wavenumber range of 200-1500 cm^{-1}. Figure 1 shows a comparison of the Raman spectra of all the types of glass used measured at the same depth. In all these spectra, we can see a band at wavenumbers between 200 and 732 cm^{-1}, which is characteristic for bending vibrations in silicate glasses.

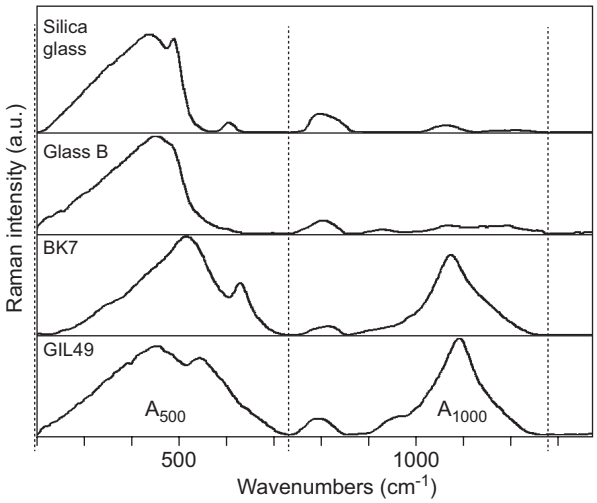

Figure 1. The Raman spectra of four types of silicate-glass substrates.

Another intensive band was found in the GIL49 and BK7 glasses at higher wavenumbers (732 - 1277 cm^{-1}). This band corresponds to stretching vibrations in glasses containing alkali oxides. In glass B and silica glass, the intensity of that band is negligible due to a low content of alkali oxides and low extent of glass structure modification. The degree of glass polymerisation was calculated as the ratio of Si–O bending (A_{500}) and stretching (A_{1000}) bands. The average value of A_{500}/A_{1000} was calculated from five spectra recorded at

different depths of the particular glass. The average values of the degree of polymerisation (A_{500}/A_{1000}) and the standard deviation of the used glasses are calculated by a standard process (see e.g. [18]) and are shown in Table 2. It is obvious that the lower degree of polymerisation corresponds to the higher content of monovalent modifiers in the glass. Such glass contains a smaller number of connected structural units [$SiO_{4/2}$] and its structure is more depolymerised. In this sense, the glass type BK7 is similar to the glass GIL49 while the structure of the glass B is silica-like glass.

Table 2. The area ratio of Si–O bending (A_{500}) and stretching (A_{1000}) bands in various types of glass substrates.

Type of glass	A_{500}/A_{1000} [–]
Silica glass	9.00 ± 0.10
Glass B	7.31 ± 0.14
BK7	1.91 ± 0.03
GIL49	1.83 ± 0.01

Changes of the glass surface structure after ion implantation

The Raman spectra of the as-implanted samples were taken from the surface to a depth of 800 nm, where no gold ions were detected by RBS [15]. The step was set to 100 nm. Simultaneously, the same measurement was done in the virgin glass substrates. At first sight, there seemed to be no differences between the Raman spectra taken from different depths as well as from implanted and non-implanted samples. Only the spectra measured at a depth of 100 nm showed a significant lower intensity of the bands for all the as-implanted samples, which could be attributed to the influence of the sample surface. Nevertheless, the evaluation of the A_{500}/A_{1000} value in the as-implanted and virgin glasses revealed glass-structure changes caused by gold implantation. In Figure 2, we can see the depth profiles of the A_{500}/A_{1000} value for the virgin and as-implanted glass. The error bars in Figure 2 are based on the standard deviations stated in Table 2. As the values that were obtained from a depth of up to 100 nm could have been influenced by the sample surface, they are not shown in Figure 2.

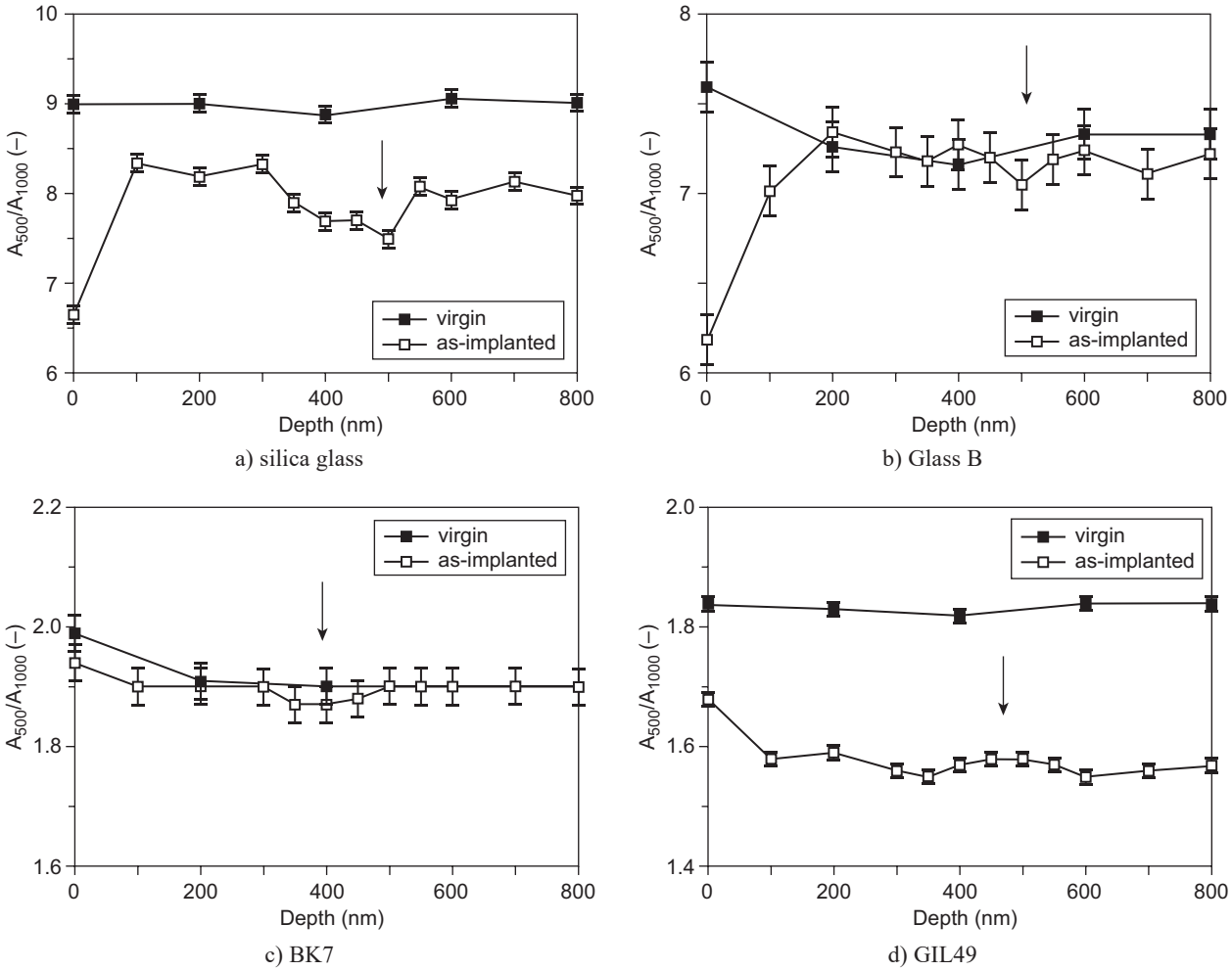

Figure 2. The depth profiles of the A500/A1000 value determined from the Raman spectra of the virgin and as-implanted silicate glasses: a) silica glass, b) Glass B, c) BK7, d) GIL49 (the crowfoots mark the concentration maximum of Au determined by the RBS analysis).

The visible drop of polymerisation degree is obvious in all of the as-implanted samples, being the most noticeable in the as-implanted silica glass (see Figure 2a) and the least detectable in the glass B. The decrease of the A_{500}/A_{1000} value (i.e. the degree of polymerisation) is the most significant at the depths corresponding well with the gold-content maximum determined from the RBS profiles. For the silica glass, the maximum of the Au concentration was found in a depth of 569 nm, for glass B in 519 nm, for GIL 49 in 515 nm and for BK7 in ≅480 nm (in the Figure 2 the concentration maximum was marked-signalized by crowfoot).

Spectral-component analysis was done only in the Raman spectra of the glasses GIL49 and BK7, where a broad stretching-vibration peak of Si–O bond appeared. Different spectral components Q_n were analysed and marked as assigned in the literature to the vibrations with zero (Q_0 or isolated SiO_4, ca 800 - 850 cm^{-1}), one (Q_1 or Si_2O_7 groups, ca 950 cm^{-1}), two (Q_2 or silicate chains, ca 1050 - 1100 cm^{-1}), three (Q_3 or sheet-like region, ca 1100 cm^{-1}) and four (Q_4, SiO_2 and tectosilicates, ca 1150 - 1250 cm^{-1}) bridging oxygen atoms per silica tetrahedral structure group. In the Raman spectra of three component glasses of the $Na_2O–B_2O_3–SiO_2$ system, it is possible to distinguish one band corresponding to the stretching vibrations of the terminal groups of silicon – oxygen tetrahedrons Q_n (800 - 1200 cm^{-1}), one band arising from the symmetrical stretching and partially deformation vibrations of Si–O–Si bridges (300 - 800 cm^{-1}) and one band corresponding to the vibrations of BO_3 triangles with one non-bridge oxygen atom in the region of the vibrations of borate groups (1200 - 1600 cm^{-1}) [20].

An example of the spectral component analysis of both glasses is shown in Figure 3. The top grey curve represents the measured Raman spectrum while the other ones represent separated bands. A comparison of the separated spectra of both glasses showed that the individual bands Q_1 and Q_4 are shifted towards the lower wavenumber in the glass BK7. Moreover, it arises from the spectrum of the BK7 glass that the bands Q_2 and Q_3 have different intensities from those in the spectrum of the glass GIL49. The percentage amount of the Q_n species was calculated as the ratio of the area of the given band Q_n and the sum of area of all the bands according to the following equation:

$$\text{percentage amount } (Q_n) = \frac{S(Q_n)}{\sum_{n=1}^{4} S(Q_n)} \cdot 100$$

where S is the area of the pertinent band Q_n.

The amount of each Q_n species was found to be constant through all the measured depths (i.e. from the surface to a depth of 800 nm) of the virgin glass.

A comparison of the depth profiles of the amount of the Q_n species in the as-implanted samples revealed interesting changes. Figure 4 shows the dependence of the Q_n values on the depth in the glasses GIL49 and BK7 before and after the implantation. The amount of the Q_2 increased in the depth range of 0 - 400 nm (i.e. at the depth with the highest concentration of gold) in the as-implanted glass GIL49, whereas the amount of Q_3 decreased at the same time (Figure 4a). For the BK7 glass, only a very small drop of the Q_4 amount was observed on the glass surface (Figure 4d). No noticeable changes of the amounts of the other Q_n species were found after the ion implantation in the glass BK7.

The glass-surface structure changes after annealing

It is well known that the annealing of the as-implanted samples significantly changes their properties. After Au^+-ion implantation, all of the types of silicate glass mentioned above were annealed under the same conditions, i.e. for 5 hours at 600°C, in the ambient atmosphere. The temperature of annealing corresponded

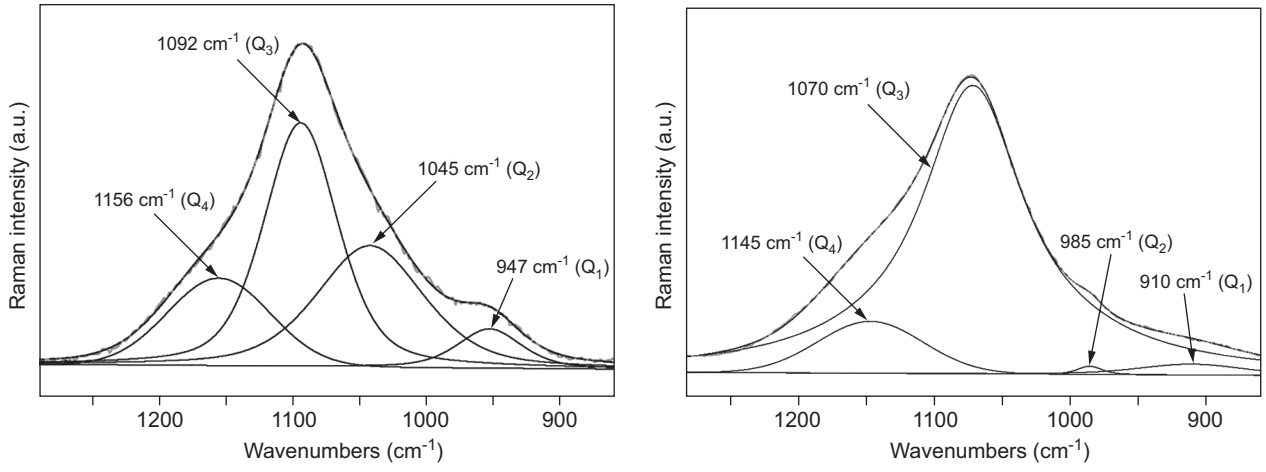

Figure 3. A spectral component analysis of the stretching-vibration band for two types of glass substrate measured at a depth of 500 nm under the surface: a) GIL49, b) BK7.

to our previous study of the annealing of the glass GIL49 [18]. When that temperature was used, the glass became stained red, which indicates the presence of gold nanoparticles in the glass. At lower temperatures, no colours were observed, whereas higher temperatures induced damage to the glass. The changes of the gold-concentration depth profiles measured by RBS in the as-annealed samples were described in [15], for silica glass in [16].

The Raman spectra of the as-annealed glasses showed a quite interesting aspect. The analysis of the spectra revealed a change of the A_{500}/A_{1000} value caused by the annealing. Except for the glass BK7, the A_{500}/A_{1000} value converged towards the value of the original glass. In GIL49, the value of A_{500}/A_{1000} was found to be higher than the one in the virgin glass, unlike in the BK7 glass, where that value decreased after annealing.

The amount of the Q_n species was evaluated using the same procedure as that mentioned above, again only for the glasses BK7 and GIL49. A comparison of the amounts of both Q_2 and Q_3 species in the glass GIL49 for virgin, as-implanted and as-annealed glasses is shown in Figure 5a, b. After annealing, the amount of the Q_2 and Q_3 species clearly approximated towards the original value of the GIL49 glass. The amount of Q_1 and Q_4 did not change much after annealing (not shown). Surprisingly, after annealing the amount of Q_1 in the BK7 glass increased as the amount of Q_3 decreased (see Figure 5c, d). A small drop in the amount of Q_4 was also observed (not shown).

DISCUSSION

The results obtained from the study of the glass structure by Raman spectroscopy can be interpreted on the basis of [13]. Ion implantation into the glass caused damage to the glass network, resulting in the breaking of the existing bonds, i.e. the so-called depolymerisation of the glass network. This depolymerisation (reduction of the A_{500}/A_{1000} value) is the most apparent in the area where the concentration of the in-implanted ion is the highest and the highest level of structural changes is expected because of the highest energy deposition per one nm caused by the ions stopped at this depth. Despite

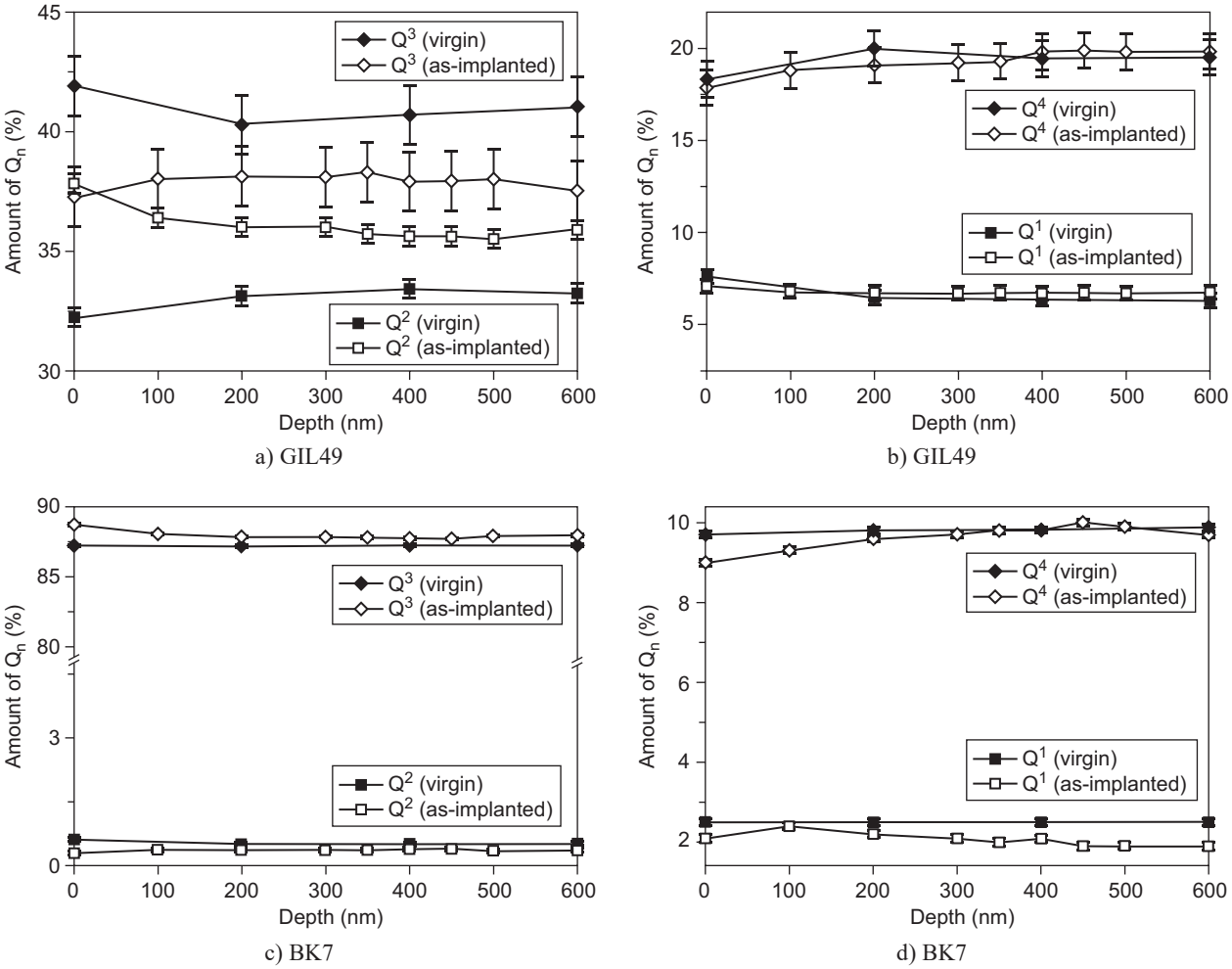

Figure 4. The depth profiles of the amount of the Qn species in the as-implanted glass: a) GIL49 – Q_3 and Q_2; b) GIL 49 – Q_1 and Q_4; c) BK7 – Q_3 and Q_2; d) BK7 – Q_1 and Q_4.

the fact that all of the glasses were implanted under the same conditions, the extent of A_{500}/A_{1000} reduction differs for the particular glasses, which implies that the degree of depolymerisation depends on the composition of the glasses, i.e. on their structure. The biggest extent of depolymerisation was exhibited by the silica glass (15 - 17 %), which is a glass with a very high amount of cross-linking, and that is why Raman spectroscopy, particularly in this glass, is very sensitive to any changes concerning the internal arrangement of the bonds.

On the contrary, the glass BK7 revealed the smallest degree of depolymerisation after the ion implantation. The boron-silicon network seems to be more sensitive to ion implantation than silicate. We suppose that ion implantation means the breaking of such bonds as B–O rather than Si–O bonds. According to [19], the strength of the field around Si is higher than that around B, which means that the Si–O bond is stronger than B–O, which has confirmed our hypothesis that during implantation are the first to break the weaker B–O bonds.

Depolymerisation appeared also after the separation of the stretching (Si–O) vibration bands in the Raman spectra. The increment of the amount of Q_2 after the ion implantation is indicates of the increased number of NBO atoms in the glass. Q_2 species represent a silicon atom bearing two NBO and two BO atoms. Subsequently, this means that the glass structure contains the following chains:

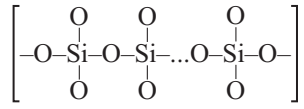

The amount of Q_3 decreases, thus increasing the Q_2 and Q_4 values. The fact that in the BK7 glass the changes of the Q_n species were not as apparent as in the GIL49 glass may be taken as evidence that ion implantation preferably causes the breaking of the glass network in the vicinity of boron rather than in a much less afflicted neighbourhood of silicon.

The differences between the particular glasses which were implanted by high-energy Au^+ ions became apparent also after the post-implantation annealing. RBS concentration depth profiles showed that gold migrated through the various glass matrixes differently [15, 16]. This may be caused by several factors, e.g. by the different extent of depolymerisation after the

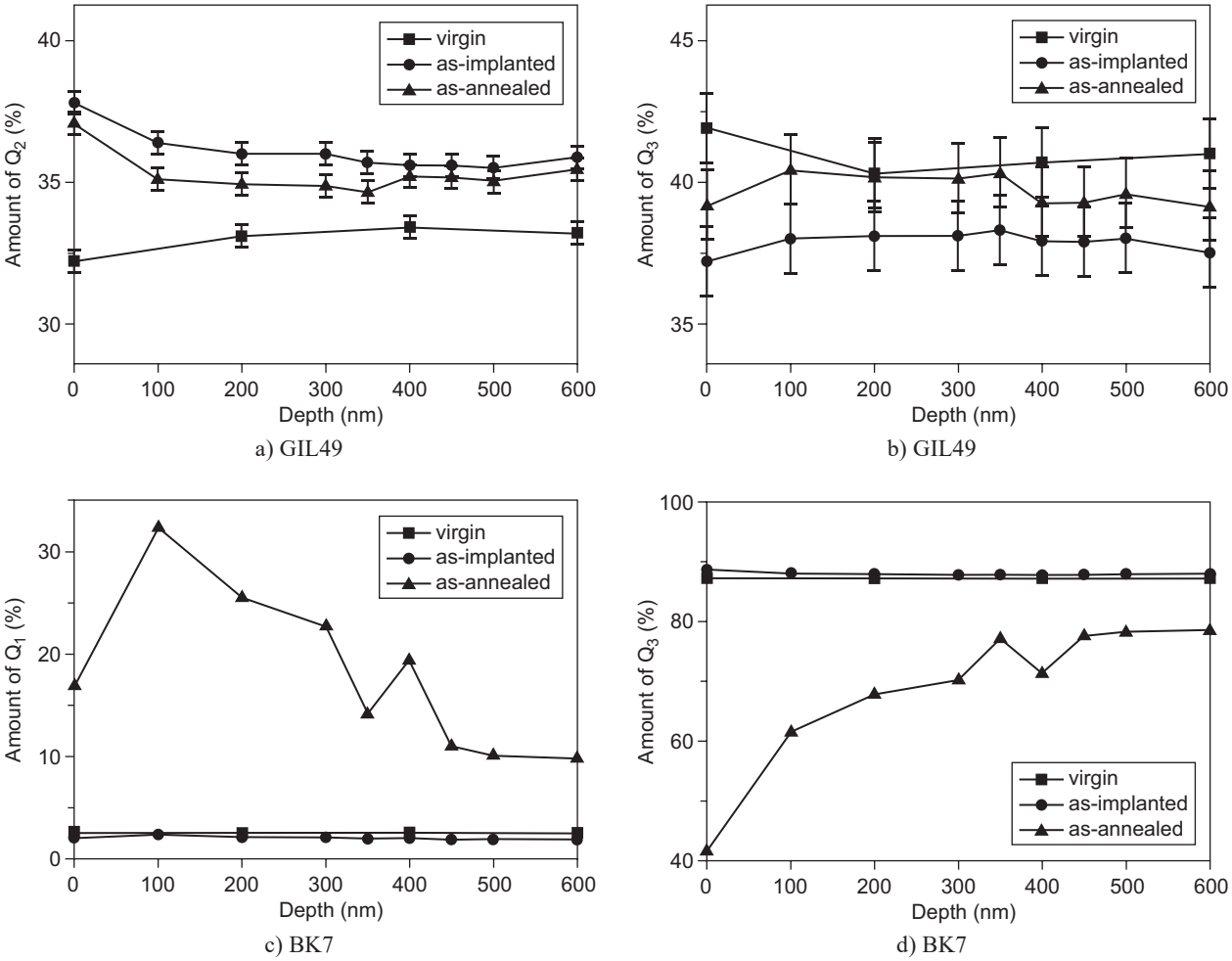

Figure 5. The depth profiles of the amount of the Q_n species in the as-annealed samples: a) GIL49 – Q_2; b) GIL 49 – Q_3; c) BK7 – Q_1; d) BK7 – Q_3 .

implantation, subsequently by the different recovering rate of the glass structure and the formation of new bonds; nevertheless, it may also be connected with the temperature of annealing.

Allow us to consider what may happen with the structure of glass during annealing. The annealing made a shift of the A_{500}/A_{1000} towards higher values in all of the glasses with the exception of the BK7 glass. This might mean that in the former glasses the annealing caused the creation of new areas with a lesser extent of depolymerisation during the ion implantation in contrast to the BK7 glass, where the annealing caused an even bigger extent of depolymerisation than that which occurred after the implantation.

CONCLUSION

It was confirmed that Raman spectroscopy is a suitable tool for determining the degree and extent of the so-called depolymerisation of the glass network after ion implantation. From the Raman spectra, it is also possible to determine the recovering process rate of the glass structure during the post-implantation annealing. Annealing made it possible for the glass structure damaged by the implantation to recover, which included the formation of new bonds, nucleation and creation of nanoparticles. The formation of new bonds was also confirmed by Raman spectroscopy. The degree of depolymerisation and the rate of recovery are affected by the glass structure; this means that the composition of the glass is a very important factor.

Acknowledgments

The research has been realised at the CANAM (Center of Accelerators and Nuclear Analytical Methods) infrastructure and has been supported by project No. P108/12/G108.

REFERENCES

1. Gleiter H.: Prog. Mater. Sci. *33*, 223 (1989).
2. Suryanarayana C., Froes F.H.: Met. Trans. *23A,* 1071 (1992).
3. Ed. Rimini E.: *Ion Implantation: Basics to Device Fabrication*, Kluvert Academic, 1994.
4. Townsend P.D., Chandler P.J., Zhang L.: *Optical Effects of Ion Implantation*, Cambridge University Press, 1994.
5. Eds. Gupta M.C., Ballato J.: *Handbook of Photonics*, CRC Press, New York, 2006.
6. Gonella F.: Rev. Adv. Mater Sci. *14*, 134 (2007).
7. Mazzoldi P., Mattei G.: Phys. Stat. Sol. (a) *204*, 621 (2007).
8. Amekura H., Plaskin O.A., Kono K., Takeda Y., Kiskimoto N.: J. Phys. D: Appl. Phys. *39*, 3659 (2006).
9. Eds. Kasap S., Capper P.: *Springer Handbook of Electronic and Photonic Materials*, p. 1063–1074, Springer 2006.
10. Colomban P.: J. Non-Cryst. Solids *323*, 180 (2003).
11. Bach H., Neuroth N.: *The Properties of Optical Glass*, Springer – Verlag, Berlin 1998.
12. Rao K.J.: *Structural Chemistry of Glasses*, 1st ed., Elsevier, 2002.
13. Schultz-Münzenberg C.: *How to describe the topological structure of glasses*, Springer, Berlin Heidelberg, 1999.
14. Malinský P., Macková A., Nekvindová P., Švecová B., Kormunda M. et al. in: AIP Conf. Proc. *1412*, 327 (2011).
15. Malinsky P., Mackova A., Bocan J., Svecova B., Nekvindova P.: Nuclear Instr. Meth. Phys. Res. B 267 (2009).
16. Svecova B., Nekvindova P., Mackova A., Malinsky P., Janecek M., Pesicka J., Spirkova J.: "*The effect of various silicate-glass matrixes on gold-nanoparticle formation"*; in process of preparation for publication (Journal Opt. Adv. Mat.)
17. Husinsky W., Ajami A., Nekvindova P., Svecova B., Pesicka J. and Janecek M.: Optics Comm. *285*, 2729 (2012).
18. Svecova B., Nekvindova P., Mackova A., Malinsky P., Kolitsch A., Machovic V., Stara S., Mika M., Spirkova J.: J. Non-Cryst. Sol. *356*, 2468 (2010).
19. Volf M.B.: *Chemie skla*, SNTL, Praha 1978.
20. Koroleva O.N. et al.: Glass and Ceramics *67*, 340 (2011).